A new comprehensive framework for probabilistic tractography of fanning fibres

J. Campbell[1], P. MamayyezSiahkal[2], P. Savadjiev[3], I. R. Leppert[1], K. Siddiqi[2], and G. B. Pike[1]
[1]McConnell Brain Imaging Centre, Montreal Neurological Institute, McGill University, Montreal, Quebec, Canada, [2]Centre for Intelligent Machines, McGill University, [3]Brigham and Women's Hospital, Harvard University

Introduction: The objective of the current work was to develop an improved probabilistic tractography framework that could handle, in addition to crossing fibres, information on more complex subvoxel geometries, such as fanning fibres [1]. The technique incorporates a residual bootstrap probabilistic processing step [2,3,4], followed by a tractography process that results in the assignment of an index of connectivity, at each voxel in the volume, to the region of interest (ROI) of the user's choice. This connectivity index is derived using a *weakest link* approach [5,6], and solves many of the problems inherent in popular connectivity indices that are based on *frequency of connection* [7,8].

Methods: ***MRI acquisition:*** Sample MRI data were acquired for one healthy subject on a Siemens 3T Trio MR scanner (Siemens Medical Systems, Erlangen, Germany) using an 8-channel phased-array head coil. Diffusion encoding was achieved using a single-shot spin-echo echo planar sequence with twice-refocused balanced diffusion gradients. A dataset designed for high angular resolution reconstruction was acquired with 99 diffusion encoding directions, 2 mm isotropic voxel size, 63 slices, b=3000 s/mm^2, TE=121 ms, TR=11.1 s, and GRAPPA parallel reconstruction. A 1 mm isotropic resolution T1 weighted anatomical scan was also acquired.

Bootstrap probabilistic deconvolution: The diffusion weighted signal profiles were fitted to a spherical harmonic basis of order eight. A residual bootstrap algorithm similar to approaches described recently for probabilistic high angular resolution diffusion imaging [3,4,9] was run using 100 iterations. For each iteration, the new signal profile was input to a spherical deconvolution algorithm. The deconvolved ODFs were used as input to a curve inference algorithm [1], which outputs a description of the subvoxel geometries present in each voxel. The result of this process is that each voxel is assigned a probability of containing a single fibre, a double crossing, a triple crossing, or a fanning fibre configuration. For each geometry, the mean orientation and the standard deviation of the distribution of directions is output, as well as vectors describing the extent and polarity of the fanning fibres in the case of fanning (see Fig. 1).

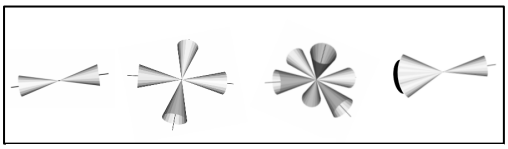

Fig.1 Complex subvoxel fibre geometries, including subvoxel fanning, and their cones of uncertainty.

Weakest link probabilistic tractography: Tractography was achieved by iterative streamline propagation starting from one or more user-defined ROIs. At each step, the direction of propagation is chosen from within the cone subtending one standard deviation of the distribution of fibre directions. The confidence in the direction of propagation is given by the corresponding value of this distribution. The confidence in any streamline is given by the lowest confidence value for all segments along the streamline (see Fig. 2). The connectivity index for any voxel to a user-defined reference ROI is given by the highest confidence value of all tracts that connect that voxel to the reference ROI. Note that for fanning, a constant high confidence is assigned for the entire extent of the mean fan. The tracking experiments were run twice, once without the incorporation of fanning information, and once with fanning.

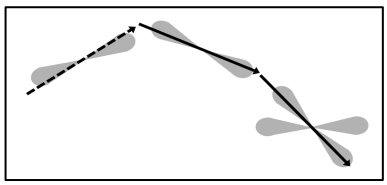

Fig.2 The weakest link connectivity index assigns the lowest segment confidence value (dashed line) to the entire tract.

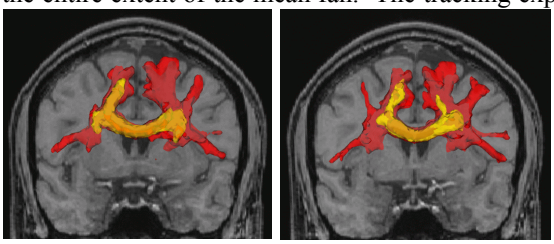

Fig.3 Tracking result in the corpus callosum. The red surface outlines the full extent of the voxels reached, and the yellow surface outlines a high-confidence level set in the connectivity index map. *Left*: no fanning; *Right*: using fanning information.

Results and Discussion: Fig. 3 shows the tractography result for one multi-voxel seed and reference ROI placed in the centre of the corpus callosum. Two major differences were observed between the tractography with and without fanning. First, the total extent of the voxels reached is slightly greater in the case of fanning: while the major fibre pathways remain the same, the fanning allows the tractography to reach gyri missed in the non-fanning case. Second, within the subset of voxels reached by both approaches, the fanning approach leads to more accurate assignment of the connectivity index due to the more accurate description of the geometry: the higher confidence region extends further toward the cortex than in the non-fanning case. In the case of fanning, these voxels were reached by propagating within the fan, where all confidence values are high. Without fanning information, the same voxels were reached by propagating near the edge of the cone of uncertainty for a single fibre, where the confidence values are low.

The *weakest link* connectivity index has several features to note, in comparison to more frequently used *frequency of connection* connectivity indices [7,8]. First, the connectivity index map is monotonic: it is impossible for a voxel to be more connected to the reference ROI than is any intermediate voxel. Second, the confidence values obtained with the weakest link approach are independent of the size and shape of the tract-delineating ROIs, which is not the case with the frequency of connection approach, where "hot spots" can occur. Third, the weakest link approach is less corrupted by distance effects, which give a strong bias to shorter connections in the frequency of connection approach.

References & Acknowledgements: [1] Savadjiev *et al*. MedIA 10 (2006): 799–813. [2] Jones *et al*. MRM 49 (2003): 7-12. [3] Berman *et al*. NeuroImage 39 (2008): 215-22. [4]Jeurissen *et al*. HBM (2010): 1093-97. [5] Parker *et al*. TMI 21 (2002): 505-12. [6] Campbell *et al*. NeuroImage 27 (2005):725-36. [7] Parker *et al*. JMRI 18 (2003): 242-254. [8] Behrens *et al*. MRM 50 (2003): 1077-88. [9] Haroon *et al*. OHBM (2007): 273. This work was supported by NSERC Canada.